Accepted to Phys. Fluids 10.1063/5.0134307

Wall Repulsion during Electrophoresis: Testing the theory of Concentration-Polarization Electroosmosis

Raúl Fernández-Mateo,[1] Hywel Morgan,[1] Antonio Ramos,[2] and Pablo García-Sánchez[2]
[1)]*School of Electronics and Computer Science, University of Southampton, Southampton SO17 1BJ, United Kingdom.*
[2)]*Depto. Electrónica y Electromagnetismo. Facultad de Física. Universidad de Sevilla. Avda. Reina Mercedes s/n, 41012. Sevilla (Spain).*

(*Electronic mail: r.fernandez-mateo@soton.ac.uk)

(Dated: 21 December 2022)

We experimentally study the repulsion of charged microscopic particles with the channel walls during electrophoresis in microfluidic devices. For low frequencies of the electric fields ($< 10\,$kHz), this repulsion is mainly due to the hydrodynamic interaction caused by the flow vortices that arise from the slip velocity induced by the electric field on the particle surface, as shown in a recent publication [Fernandez-Mateo et al., *Physical Review Letters*, **128**, 074501, (2022)]. The maximum slip velocity on the particle surface is inferred from measurements of wall-particle separation. Importantly, this procedure allows us to infer very small slip velocities that otherwise are too weak to be measured directly. Data at small electric field amplitudes (E_0) agree with theoretical predictions using the model of Concentration Polarization Electroosmosis (CPEO), which has recently been proposed as the mechanism behind the flow vortices on the surface of the particles. Data for higher electric fields show that the predictions of the CPEO theory for weak electric fields are not valid beyond $E_0 \sim 60$ kV/m. Additionally, we also show that, for sufficiently strong electric fields, the quadrupolar flow structures become disrupted, leading to a weaker wall repulsion.

I. INTRODUCTION

Electrophoresis is the motion of charged colloidal particles suspended in an aqueous electrolyte when subjected to a uniform electric field[1]. Particles are usually suspended in an aqueous electrolyte so that the surface charge is screened by a diffuse ionic layer, giving rise to an electrical double layer (EDL). The action of an external electric field $\mathbf{E}$ on the EDL leads to a relative motion between the liquid and the particle. When the diffuse ionic layer is thin compared to particle size, the velocity of the particles $\mathbf{u}$ is given by the Helmholtz-Smoluchowski formula[2]

$$\mathbf{u} = \frac{\varepsilon\zeta}{\eta}\mathbf{E} \tag{1}$$

where ε and η are the electrolyte permittivity and viscosity, respectively and ζ is the zeta potential of the particle-electrolyte interface. The latter is generally considered to be the electrical potential at the inner edge of the diffuse ionic layer surrounding the particle[1].

Practical applications of electrophoresis typically make use of capillaries and/or microchannels that contain the liquid and suspended particles. Several studies have shown that particles undergoing electrophoresis are repelled from the neighbouring dielectric walls of the channel[3,4]. These early studies reported the lateral migration of particles in dc electric fields. However, a simple symmetry argument[5] leads to the conclusion that the effect cannot be due to classical electrophoresis, meaning that particle-wall repulsion is independent of the orientation of the field. Thus, the use of ac electric fields to examine the particle-wall interaction provides a simpler scenario to test experimental results against theoretical predictions given that it provides a decoupling from the two phenomena of particle electrophoresis and electroosmosis.

Recently, we have shown that for the case of a low-frequency ac electric field ($< 10\,$kHz), repulsion is due to the hydrodynamic wall-particle interaction that arises from the fluid flow induced by the electric field around the particle[5]. This contrasts with previous publications that explain the origin of the particle-wall repulsion as the electrostatic interaction between the electrical dipole induced on the particle and its image dipole in the wall[6]. The measured particle-wall separation was in agreement with the observed quadrupolar flow structures around charged microspheres when suspended in low-conductivity electrolytes, and could be satisfactorily explained by classical dipole-dipole repulsion in the case of higher frequencies and electrolyte conductivities[5].

The quadrupolar flows shown in Figure 1 are caused by Concentration-Polarization Electroosmosis (CPEO)[7], i.e. stationary electrosmotic flow arising from variations in the electrolyte concentration around dielectric particles that occurs because of surface conduction[8]. The results in ref. 5 demonstrated a correlation between measurements of the velocity magnitude of the quadrupolar flows around the particles and measurements of the particle-wall separation, regardless of the physical origin of the flows. The goal of this paper is to compare experimental data of particle-wall separation with the theoretical predictions from CPEO theory.

The general theory for CPEO flows is only valid in the limit of weak electric fields[9]. In other words the product of the electric field magnitude (E_0) and particle radius (a) must be of the order or smaller than the *thermal voltage*[10] ($E_0 a < k_B T/e \approx 25\,$mV, where k_B is Boltzmann's constant, T the absolute temperature and e the proton charge). This criterion was not met in our previous experiments in ref. 5 where

Accepted to Phys. Fluids 10.1063/5.0134307

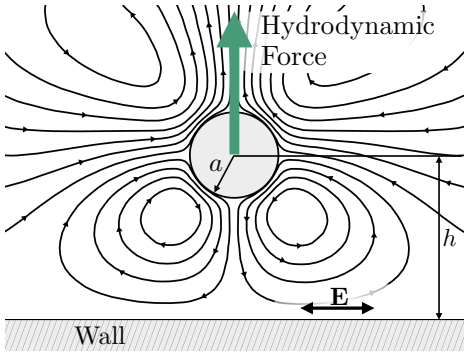

FIG. 1. Schematic representation of the streamlines for the stationary quadrupolar fluid flow around a spherical particle near a flat wall when an ac electric field is applied in the direction parallel to the wall. The resulting force appearing on the particle is marked by the green arrow.

we used particles with diameters between 1 and 3 microns subjected to ac fields with an amplitude of $E_0 = 80\,\text{kV/m}$. In this paper we present experimental data of wall-particle separation for a wide range of electric field amplitudes. Specifically particle-wall repulsion data at small electric fields provide a quantitative comparison with the theoretical model, whilst data at higher electric fields define the limits of applicability of the current CPEO theory. In the range of electric field magnitudes where the effect of wall repulsion during electrophoresis is dominant, i.e. from ∼10 kV/m to ∼100 kV/m, particles between 1 μm and 3 μm provide a good range for $\beta = eE_0a/(k_BT)$: from β = 0.2 (in the linear regime), up to $\beta > 6$ where deviations from CPEO are expected. In order to compare with theory, the experimental data for particle-wall separation was used to extract the slip velocity on the surface of the particle, and these velocities were then compared to theoretical prediction. Remarkably, this procedure allows us to deduce very small slip velocities on particles that are otherwise too small to be measured directly. We also show that for sufficiently strong electric fields, the quadrupolar flows become disrupted, leading to weaker wall repulsion.

II. EXPERIMENTAL DETAILS

Electrophoresis experiments were performed with microchannels 1 cm long and 50×50 μm square cross-section – see Figure 2. Channels were made from polydimethylsiloxane (PDMS) using standard soft-lithography and bonded to a glass wafer. They were pre-treated with a non-ionic surfactant (Pluronic F-127) to avoid non-specific particle adhesion to the walls. A side-effect of this treatment is that electroosmosis on the channel walls is very much reduced[11,12]. The following particles were used: fluorescent carboxylate particles of 1 μm, 2 μm, and 3 μm diameter, along with plain polystyrene particles of 3 μm diameter. The latter particles have a lower surface charge than that of the carboxylate particles. The zeta-potentials of the particles were measured using a Malvern Zetasizer, resulting in -62 mV for the 1 μm particles, -72 mV for the 2 μm particles, -81 mV for the 3 μm carboxylate particles and -27 mV for the 3 μm plain particles. All particles were suspended in KCl solutions at 1.7 mS/m conductivity.

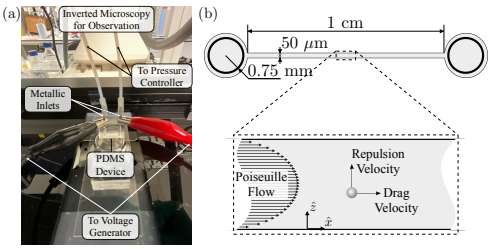

FIG. 2. (a) Photograph of the experimental set-up with the microfluidic device made of PDMS and plasma-bonded to a glass slide. The metallic inlets of the device are connected to a pressure controller and clips to apply the voltage signal. Particle movement was measured with an inverted microscope. (b) Drawing of the microfluidic channel (not to scale) and a diagram showing the particles flowing in a Poiseuille profile while being repelled from the channel walls.

The electric field along the channel was applied to two metal needles inserted into the reservoirs at each end. Electric fields were generated with amplitudes from 10 kV/m up to 100 kV/m and frequencies ranging from 50 Hz to 10 kHz. In a typical experiment, the particle suspension is pumped into the channel through one of the needles using a pressure generator to maintain a constant flow with an average velocity of 1.56 mm/s. The particle concentration was kept very low to avoid particle-particle interactions so that they flow through the channel one by one. Videos of particle motion were captured with a camera connected to the microscope and the particle positions in the transverse direction to the fluid flow were determined using a custom-written Matlab code[5].

III. EXPERIMENTAL RESULTS

In order to visualize the particle distribution across the channel, we recorded movies containing more than 600 frames which were later stacked, resulting in composite images where showing all the particles that appeared throughout the full duration of the video at once. This clearly shows the depletion regions near the channel walls, which is not related to the particle concentration in the electrolyte. Figure 3 shows the example of 3 μm carboxylate particles driven by a Poiseuille flow and subjected to an electric field of multiple amplitudes and 90 Hz of frequency. It shows that prior to the application of the electric field, particles were randomly

distributed in the channel (left-most image). As shown in the figure, the stream of particles becomes focused as the electric field intensity increases, leading to the regions devoid of particles near the channel walls.

Particle separation was characterized by measuring the regions devoid of particles. This was quantified by making a histogram of the transverse coordinates of the particles, i.e. the distance of a particle to one of the channel walls $z_i, i \in (1,..,N)$, where N is the total number of particles. The wall separation is then defined as the width of the depletion zone, calculated as half the difference between the channel width and the width of the z_i histogram (this width is defined as the range that contains 95% of all positions).

Figure 4 shows the wall separation for carboxylate particles (3 μm diameter) as a function of the frequency of applied voltage for an electrolyte conductivity of 1.7 mS/m. In Figure 4(a) the electric field amplitude was 60 kV/m, and particles show a monotonous decrease in wall separation with frequency of the electric field, as predicted by the linear model (described in section IV). However, experimental data for higher electric fields (100 kV/m) presented in Figure 4(b) clearly show a minimum in the wall separation at around 2 kHz. This result is not predicted by the CPEO theory, where the slip velocity (and wall repulsion) varies monotonically with frequency of the electric field.

In order to clarify this result, small fluorescent tracer particles (500 nm diameter) were used to visualize the quadrupolar flow structure around individual 3 μm spheres. The insets in Figure 4(b) show example images of flow created by superimposing approximately 10 frames. These show that flow field below $\sim$ 1 kHz is distorted, while at higher frequencies the fluid flow patterns around the sphere tends to recover the expected structure.

Figure 5(a) shows the wall separation for four different particles as a function of the amplitude of the electric field for a fixed frequency of 90 Hz, whilst Figure 5(b) shows wall separation for the same conditions but a higher frequency of 527 Hz.

IV. THEORY AND COMPARISON WITH EXPERIMENTAL DATA

As mentioned above, the application of an ac field to a dispersion of charged dielectric particles leads to a well-defined pattern of electroosmotic flows driven by CPEO[9]. The time-averaged slip velocity on spherical particles can be written as $v_{\text{slip}} = v_0 \sin(2\theta)$, where θ is the polar angle with respect to an axis given by the direction of the electric field, and v_0 was derived for a sphere with arbitrary Dukhin number in a previous publication[9]. The Dukhin number, Du, is the ratio of surface conductance on the particle K_s, to the bulk conductance: $\text{Du} = K_s/(a\sigma)$, where a is the particle radius and σ is the electrical conductivity of the electrolyte[8]. A matlab script for computing the value of v_0 can be found in the Supplementary Material. This slip velocity leads to an axisymmetric flow pattern structure around the spherical particles with the symmetry axis given by the direction of the applied electric field[13]:

$$\mathbf{v}_{\text{CPEO}} = v_0 \left(\frac{(1-(r/a)^2)(1+3\cos 2\theta)}{2(r/a)^4} \hat{r} + \frac{\sin 2\theta}{(r/a)^4} \hat{\theta} \right), \quad (2)$$

where r is the radial distance. Conducting spheres suspended in electrolytes also develop quadrupolar flows as given by eq. (2) when subjected to electric fields. In this case, the slip velocity on the particle arises because of induced-charge electroosmosis (ICEO)[14]. ICEO flows are negligible for dielectric particles[7], therefore only CPEO is considered as the origin of the quadrupolar flows.

The flow patterns are distorted by the presence of nearby walls; the resulting flow structure is described by the superposition of eq. (2) and the flow field reflected from the wall (see Fig. 1). Importantly, the action of the reflected flow on the particle leads to motion away from the wall. If the particle is far from the wall, its drift velocity is given by:

$$u = v_0 \frac{3a^2}{8h^2}, \quad (3)$$

where h is the distance of the particle center to the wall. This equation is a particular case of the expression derived by Smart and Leighton[15] for the drift of a stresslet due to the presence of a plane. In the context of electrokinetics, Yariv[16] obtained this expression for the case of repulsion of conducting spheres from a wall due to ICEO quadrupolar flows.

Taking into account the expression for the repulsion velocity given in eq. (3), we obtain an analytical expression for the particle-wall separation at the end of the channel. First, consider the mid horizontal plane of the channel. This corresponds to the focal plane measured in the experiments where particles are imaged. The velocity component of the particles along the channel u_x is given by the fluid velocity on this plane, which can be approximated by a parabolic profile,

$$\mathbf{v}_{\text{Poiseuille}} = 4\mathscr{V} \left[\frac{z}{W} - \left(\frac{z}{W} \right)^2 \right] \hat{x}, \quad (4)$$

where $\mathscr{V}$ is the maximum fluid velocity in the channel, z is the transverse position to the direction of the flow measured from one of the walls, and W the channel width. This approximation (4) differs by less than 4% from the exact solution for the fully developed Poiseuille flow in the mid plane of a channel with square cross-section[17]. Since there are two side walls, the component of particle velocity perpendicular to the channel u_z results from applying eq. (3) to both walls and adding the contributions:

$$\mathbf{u_z} = v_0 \frac{3a^2}{8} \left[\frac{1}{z^2} - \frac{1}{(W-z)^2} \right] \hat{z}, \quad (5)$$

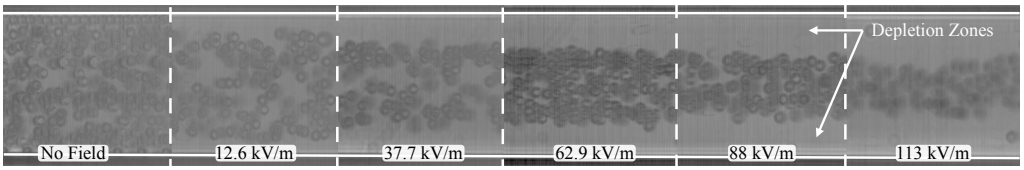

FIG. 3. Sequence of composite images from video recordings taken at the end of the channel showing 3 μm carboxylate particles flowing in a 1.7 mS/m KCl electrolyte for different electric field amplitudes, with $f = 90$ Hz. Particle-depleted regions are created near the channel walls because of particle-wall repulsion. As the field intensity increases, so does the repulsion and therefore the wall separation at the end of the channel. The apparently high concentration of particles in this image is due to image post-processing (stacking of the frames) and does not show the actual particle concentration. The channel walls are marked by the horizontal white lines, separated by 50 μm.

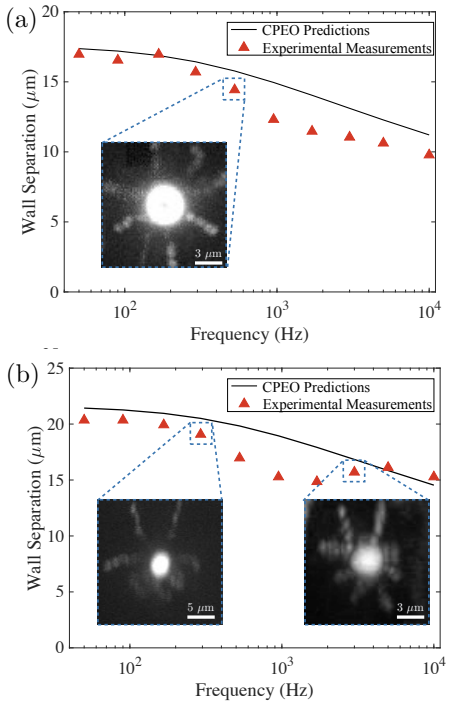

FIG. 4. Experimental data for wall repulsion at an electric field of (a) 60 kV/m and (b) 100 kV/m. 3 μm carboxylate particles were suspended in a 1.7 mS/m KCl electrolyte. The symmetrical flow vortices are destroyed at high electric fields as shown by the left-hand side inset image (292 Hz) in (b). The flow patterns are partially recovered at higher frequencies as seen in the right-hand side inset image taken at 3 kHz, or lower-intense fields as shown in the inset image of (a) taken at 527 Hz. Flows were traced with 500 nm fluorescent polystyrene particles.

Thus, $\mathrm{d}z/\mathrm{d}x = u_z/u_x$ can be integrated to obtain the following expression that relates the particle-wall separation h after covering a distance L along the channel with the slip velocity on the particle surface v_0:

$$v_0 = \frac{32}{3}\frac{\mathscr{V}W^3}{a^2L}[f(h/W) - f(z_0/W)]. \tag{6}$$

where z_0 is the initial separation from the wall and $f(\xi) = (18(1-2\xi)^2 - 9(1-2\xi)^4 + 2(1-2\xi)^6 - 12\log|1-2\xi|)/1536$. The width of the depletion region after a distance L along the channel can be estimated from eq. (6) with z_0 equal to the particle radius.

Since equation (6) is derived from eq. (3), it assumes that the remote-wall approximation is valid, i.e. higher order terms are neglected in the calculation of the velocity field reflected by the wall. The validity of this approximation was already tested in our previous work[5].

In order to compare the experimental results shown in Figure 5 with CPEO theory, a theoretical value for v_0 is determined using the experimental Zeta-potential values (section II) and the Dukhin number obtained from a typical value for surface conductance of colloids ($K_s = 1$ nS) independently of their size and surface functionalisation. This is a typical value obtained from experimental data for the electrokinetic properties of submicrometer latex particles[18–20] and is larger than the estimate obtained for K_s when using the theory of the diffuse layer[21]. The difference is attributed to the contribution to surface conductance arising from a layer of mobile ions adsorbed on the wall[19]—the so-called Stern layer. Figure 6 shows the non-dimensional wall separation h/W numerically obtained from equation (6) together with the measured values versus the reduced electric field $\beta = E_0ae/(k_BT)$.

The β parameter was used in ref. 9 to develop the theoretical predictions of the slip velocity in the limit of small electric field, $\beta < 1$. However, Figure 6 shows how the theoretical predictions are in good agreement with the experimental data of wall separation for values of β well above 1. Interestingly, comparing results for the cases (a) and (b) in the figure we note that the deviation from the theoretical predictions depends on the frequency of the applied electric field. This

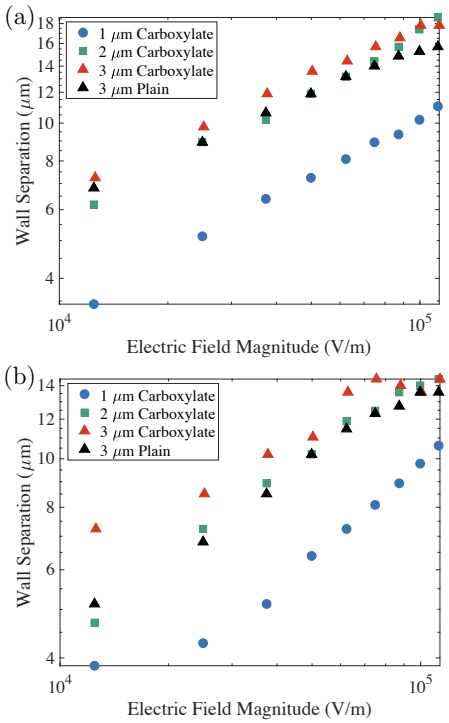

FIG. 5. Experimentally measured wall repulsion at different electric field amplitudes and two different frequencies: (a) 90 Hz and (b) 527 Hz. Four different populations of polystyrene particles suspended in a 1.7 mS/m KCl electrolyte were used: 1, 2 and 3 μm carboxylate and 3 μm plain particles.

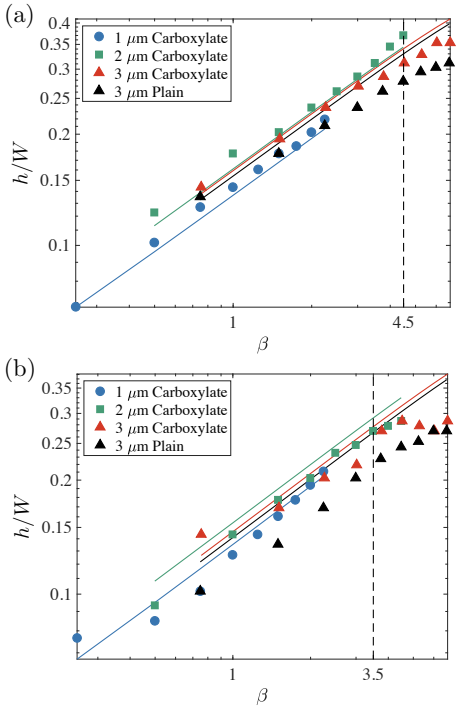

FIG. 6. Comparison of the experimental values shown in Fig. 5 with the theoretical predictions of wall repulsion from eq. (6), based on the slip velocity from CPEO theory[9]. Good agreement is seen for lower values of $\beta = E_0 ae/(k_B T)$ up to values over 1. Zeta-potential values shown in section II, $K_s = 1$ nS, with $\mathrm{Du} = K_s/(\sigma a)$. Two different frequencies are compared: (a) 90 Hz and (b) 527 Hz.

is in agreement with the data in Figure 4 which shows that the experimental data is farther from the CPEO predictions at 527 Hz than at 90 Hz. Further research will focus on understanding the upper limits of high intensity electric fields in the theory of CPEO.

V. SLIP VELOCITY ESTIMATIONS

With respect to Figure 6 it is of interest to analyze the low β regime. The agreement between theoretical predictions and experimental measurements found for low electric field amplitudes means that the slip velocity can still be related to the wall separation in this regime, as argued in ref. 5. This is significant because we are able to infer slip velocities at $\beta < 1$, something that was previously not possible using the direct measurement procedure presented in ref. 9. The reason for this is the necessity of measuring over a minimum space around the particle to trace the fluid flow. Experimentally, it was found that at least 5 radii away from the target particle is needed for the consistency of the measurements. However, as the CPEO flows decay rapidly with distance to the particle surface ($\sim (a/r)^2$), together with the fact that due to Brownian motion the velocity of 500 nm tracer particles could not be measured with velocities $<$ 2-3 μm/s, gives an approximate limit of 50 m/s below which direct experimental measurements break down.

The first reported measurements of slip velocity in ref. 9 were made using an electric field magnitude of 80 kV/m and particles of 3 μm diameter, resulting in $\beta = 4.8$. Later in ref. 5, 2 μm particles were used at the same electric field magnitude reducing β to 3.2, still far from $\beta < 1$. Although the results presented here demonstrate a good agreement for β values up to $\beta \sim 4$, thus confirming the validity of results presented previously, eq. (6) means that it is now possible

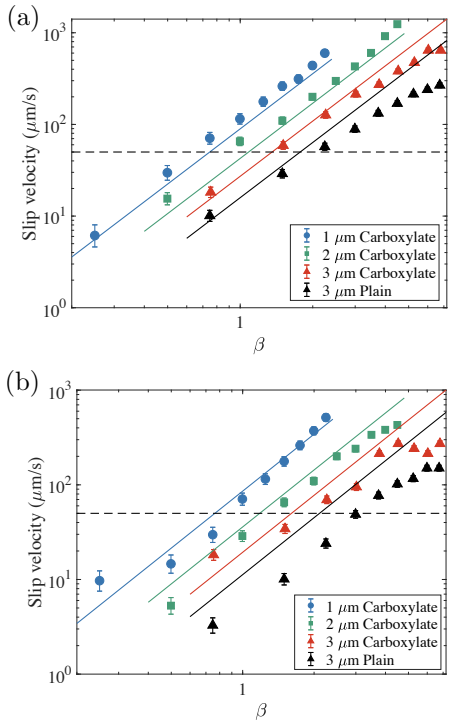

FIG. 7. Estimated slip velocity from the experimental results of wall repulsion presented in Figure 5 for the same frequencies: (a) 90 Hz and (b) 527 Hz. The horizontal dashed line marks a rough limit for the direct measurements at 50 μm/s.

to estimate the slip velocity for smaller particles and lower electric fields, where the reduced electric field is as low as $\beta = 0.2$. These results, presented in Figure 7, show a wide parametric range (electric field amplitude, frequency and particle size) of slip velocity indirect estimations.

There are several advantages to determining the slip velocity from wall repulsion measurements rather than with tracer particles. The experimental set-up is much simpler, and the measurements are automated. In other words the position of the particles in the channel is determined automatically using a custom-written software. This means that a large number of particles can be measured in a short time window, and particle-particle interaction is avoided by using low particle concentrations.

VI. DISCUSSION AND CONCLUSIONS

This paper has shown that experimental data of wall separation for dielectric microparticles undergoing electrophoresis in small electric fields ($E_0 < 60$ kV/m) agrees with theoretical predictions of the hydrodynamic interaction arising from Concentration-Polarization Electroosmosis (CPEO) around the particles. This result supports the fact that hydrodynamic forces are responsible for particle-wall separation[5] and confirms that CPEO is the mechanism behind these observed flows. Since CPEO flows around the particles are weak at small electric fields and cannot be directly measured, comparison between theory and experiments provides a further means of validating CPEO theory. Likewise, CPEO flows for small particles (less than 1 μm diameter) is very difficult to measure. Thus, this method also allows comparison between theory and experiments for colloids. Furthermore, the influence of inertial lift on electrophoresis[22] is negligible since the Reynolds number is very small in our experiments (around 0.08). This is in contrast with the experiments by Yoda et al.[23,24] where dc electrophoresis experiments combined with Pouiseuille flows show the formation of bands of colloidal particles along the direction of the flow. In those experiments, inertial lift seems to play a major role in the band formation[25]. Nevertheless, CPEO flows might also influence the band formation as in the case of the patterns of colloidal particles reported in ref. 26.

In this work the electric field can reach 100 kV/m, therefore electrothermal effects could occur in the device because temperature changes cause variations in fluid properties such as viscosity, permittivity and conductivity, and large temperature gradients can give rise to electrothermal flows[27,28]. We consider the energy balance in our system which is given by the integral form of the convection-diffusion equation with a source coming from Joule heating:

$$\rho C_p \int_V dV\,(\mathrm{v}\cdot\nabla T) - \kappa \oint_S d\mathrm{S}\cdot\nabla T = \int_V dV\,\sigma E^2, \qquad (7)$$

Here ρ is the mass density, C_p the heat capacity at constant pressure, T the temperature field and κ the thermal conductivity.

For simplicity, consider a cylindrical channel of radius $R = 25$ μm, length $L = 1$ cm surrounded by a PDMS wall with a thickness of $W = 5$ mm. The reason for considering the PDMS and not the glass side is because glass has a higher thermal conductivity (see Table S2 of the SM) and a smaller thickness. The heat flux from the convection term leads to a temperature rise of the order of $\Delta T = \sigma E_{\mathrm{rms}}^2 L/(\rho C_p v) \sim 25$ K. However, the temperature rise given by the conduction term leads to $\Delta T = \sigma E_{\mathrm{rms}}^2 R^2 \ln(W/R)/(2\kappa) \sim 0.1$ K, estimated by solving the conduction contribution of eq. (7) in cylindrical coordinates for the highest field of $E_0 = 100$ kV/m. Therefore, the heat loss due to conduction dominates, as usual in microfluidics. Moreover, this is the temperature increase with respect to the environment and not within the electrolyte in the channel, meaning that any temperature gradients in the electrolyte that could give rise to electrothermal effects are

negligible. A detailed COMSOL simulation of the system is provided in the Supplementary Material. The fully coupled fluid dynamic, electric and heat transfer problems were solved demonstrating an even lower temperature increase of just 35 mK.

Data for wall repulsion of particles at higher electric fields shows that the predictions of the CPEO theory for weak electric fields are valid up to $E_0 a \approx 4k_B T/e$, although the original framework assumed validity up to the thermal voltage $k_B T/e$. For higher electric field magnitudes, wall repulsion deviates from the expected behavior and does not monotonously decrease with frequency. The origin of these unexpected trends was clarified by visualizing the streamlines around the particles indicating that the quadrupolar flows structures become disrupted at higher electric fields, leading to a weaker wall repulsion. Finally, the influence of wall repulsion during particle electrophoresis is critical in the design of microfluidic devices that use electric fields for particle manipulation and separation[29]. Examples of use of low frequency electric fields for particle manipulation are Deterministic Lateral Displacement[30], insulating DEP[31,32] and colloidal assembly[33].

SUPPLEMENTARY MATERIAL

Supplementary Material is available at (...). This includes a detailed description of how to compute the maximum slip velocity on the surface of a sphere based on the CPEO model described in ref. 9. We also provide simulations to estimate any possible heating that might occur for the worst-case scenario, with highest electric field demonstrating that any thermal effects are negligible.

ACKNOWLEDGMENTS

PGS and AR acknowledge Grant PGC2018-099217-B-I00 funded by MCIN/AEI/ 10.13039/501100011033 and by "ERDF A way of making Europe".

DATA AVAILABILITY STATEMENT

The data that support the findings of this study are openly available in University of Southampton repository at http://doi.org/[doi].

[1]R. Hunter, *Introduction to Modern Colloid Science* (Oxford University Press, 1993).
[2]M. von Smoluchowski, "Contribution à la théorie de l'endosmose électrique et de quelques phénomènes corrélatifs," Bull. Akad. Sci. Cracovie. **8**, 182–200 (1903).
[3]L. Liang, Y. Ai, J. Zhu, S. Qian, and X. Xuan, "Wall-induced lateral migration in particle electrophoresis through a rectangular microchannel," Journal of colloid and interface science **347**, 142–146 (2010).
[4]Z. Liu, D. Li, Y. Song, X. Pan, D. Li, and X. Xuan, "Surface-conduction enhanced dielectrophoretic-like particle migration in electric-field driven fluid flow through a straight rectangular microchannel," Physics of Fluids **29**, 102001 (2017).
[5]R. Fernández-Mateo, V. Calero, H. Morgan, P. García-Sánchez, and A. Ramos, "Wall repulsion of charged colloidal particles during electrophoresis in microfluidic channels," Phys. Rev. Lett. **128**, 074501 (2022).
[6]E. Yariv, ""force-free" electrophoresis?" Physics of fluids **18**, 031702 (2006).
[7]V. Calero, R. Fernández-Mateo, H. Morgan, P. García-Sánchez, and A. Ramos, "Stationary electro-osmotic flow driven by ac fields around insulators," Physical Review Applied **15**, 014047 (2021).
[8]J. Lyklema, *Fundamentals of Interface and Colloid Science* (Academic Press Limited, 1995).
[9]R. Fernández-Mateo, P. García-Sánchez, V. Calero, H. Morgan, and A. Ramos, "Stationary electro-osmotic flow driven by ac fields around charged dielectric spheres," Journal of Fluid Mechanics **924** (2021).
[10]O. Schnitzer and E. Yariv, "Macroscale description of electrokinetic flows at large zeta potentials: nonlinear surface conduction," Physical Review E **86**, 021503 (2012).
[11]M. Viefhues, S. Manchanda, T.-C. Chao, D. Anselmetti, J. Regtmeier, and A. Ros, "Physisorbed surface coatings for poly (dimethylsiloxane) and quartz microfluidic devices," Analytical and bioanalytical chemistry **401**, 2113 (2011).
[12]R. Fernández-Mateo, P. García-Sánchez, V. Calero, A. Ramos, and H. Morgan, "A simple and accurate method of measuring the zeta-potential of microfluidic channels," Electrophoresis **43**, 1259–1262 (2022).
[13]N. I. Gamayunov, V. A. Murtsovkin, and A. S. Dukhin, "Pair interaction of particles in electric field. 1. features of hydrodynamic interaction of polarized particles," Colloid J. USSR (Engl. Transl.) **48**, 197–203 (1986).
[14]M. Z. Bazant and T. M. Squires, "Induced-charge electrokinetic phenomena: theory and microfluidic applications," Physical Review Letters **92**, 066101 (2004).
[15]J. R. Smart and D. T. Leighton Jr, "Measurement of the drift of a droplet due to the presence of a plane," Physics of Fluids A: Fluid Dynamics **3**, 21–28 (1991).
[16]E. Yariv, "Boundary-induced electrophoresis of uncharged conducting particles: remote wall approximations," Proceedings of the Royal Society A: Mathematical, Physical and Engineering Sciences **465**, 709–723 (2009).
[17]H. Bruus, *Theoretical microfluidics*, Vol. 18 (Oxford university press, 2007).
[18]W. Arnold, H. Schwan, and U. Zimmermann, "Surface conductance and other properties of latex particles measured by electrorotation," Journal of Physical Chemistry **91**, 5093–5098 (1987).
[19]V. Shilov, A. Delgado, F. Gonzalez-Caballero, and C. Grosse, "Thin double layer theory of the wide-frequency range dielectric dispersion of suspensions of non-conducting spherical particles including surface conductivity of the stagnant layer," Colloids and Surfaces A: Physicochemical and Engineering Aspects **192**, 253–265 (2001).
[20]I. Ermolina and H. Morgan, "The electrokinetic properties of latex particles: comparison of electrophoresis and dielectrophoresis," Journal of colloid and interface science **285**, 419–428 (2005).
[21]A. V. Delgado, F. Gonzalez-Caballero, R. Hunter, L. Koopal, and J. Lyklema, "Measurement and interpretation of electrokinetic phenomena (iupac technical report)," Pure and Applied Chemistry **77**, 1753–1802 (2005).
[22]V. Lochab and S. Prakash, "Combined electrokinetic and shear flows control colloidal particle distribution across microchannel cross-sections," Soft Matter **17**, 611–620 (2021).
[23]N. Cevheri and M. Yoda, "Electrokinetically driven reversible banding of colloidal particles near the wall," Lab on a Chip **14**, 1391–1394 (2014).
[24]M. Rossi, A. Marin, N. Cevheri, C. J. Kähler, and M. Yoda, "Particle distribution and velocity in electrokinetically induced banding," Microfluidics and nanofluidics **23**, 1–9 (2019).
[25]A. J. Yee and M. Yoda, "Observations of the near-wall accumulation of suspended particles due to shear and electroosmotic flow in opposite directions," Electrophoresis **42**, 2215–2222 (2021).
[26]F. Katzmeier, B. Altaner, J. List, U. Gerland, and F. C. Simmel, "Emergence of colloidal patterns in ac electric fields," Physical Review Letters **128**, 058002 (2022).

[27] A. Castellanos, A. Ramos, A. González, N. G. Green, and H. Morgan, "Electrohydrodynamics and dielectrophoresis in microsystems: scaling laws," Journal of Physics D: Applied Physics **36**, 2584–2597 (2003).
[28] Q. Wang, N. N. Dingari, and C. R. Buie, "Nonlinear electrokinetic effects in insulator-based dielectrophoretic systems," Electrophoresis **38**, 2576–2586 (2017).
[29] C. Thomas, X. Lu, A. Todd, Y. Raval, T.-R. Tzeng, Y. Song, J. Wang, D. Li, and X. Xuan, "Charge-based separation of particles and cells with similar sizes via the wall-induced electrical lift," Electrophoresis **38**, 320–326 (2017).
[30] V. Calero, P. Garcia-Sanchez, C. Honrado, A. Ramos, and H. Morgan, "Ac electrokinetic biased deterministic lateral displacement for tunable particle separation," Lab on a Chip **19**, 1386–1396 (2019).
[31] E. B. Cummings and A. K. Singh, "Dielectrophoresis in microchips containing arrays of insulating posts: theoretical and experimental results," Analytical chemistry **75**, 4724–4731 (2003).
[32] R. Fernández-Mateo, V. Calero, H. Morgan, A. Ramos, and P. García-Sánchez, "Concentration–polarization electroosmosis near insulating constrictions within microfluidic channels," Analytical Chemistry **93**, 14667–14674 (2021).
[33] M. Trau, D. A. Saville, and I. A. Aksay, "Assembly of colloidal crystals at electrode interfaces," Langmuir **13**, 6375–6381 (1997).